

Spin-orbital coupling in a triplet superconductor–ferromagnet junction

Paola Gentile,^{1,2} Mario Cuoco,^{1,2} Alfonso Romano,^{1,2} Canio Noce,^{1,2} Dirk Manske,³ and P. M. R. Brydon⁴

¹*SPIN-CNR, I-84084 Fisciano (Salerno), Italy*

²*Dipartimento di Fisica “E. R. Caianiello”, Università di Salerno, I-84084 Fisciano (Salerno), Italy*

³*Max-Planck-Institut für Festkörperforschung, Heisenbergstr. 1, D-70569 Stuttgart, Germany*

⁴*Institut für Theoretische Physik, Technische Universität Dresden, D-01062 Dresden, Germany*

(Dated: August 30, 2012)

We study a novel type of coupling between spin and orbital degrees of freedom which appears at triplet superconductor-ferromagnet interfaces. Using a self-consistent spatially-dependent mean-field theory, we show that increasing the angle between the ferromagnetic moment and the triplet vector order parameter enhances or suppresses the p -wave gap close to the interface, according as the gap antinodes are parallel or perpendicular to the boundary, respectively. The associated change in condensation energy establishes an orbitally-dependent preferred orientation for the magnetization. When both gap components are present, as in a chiral superconductor, we observe a first-order transition between different moment orientations as a function of the exchange field strength.

PACS numbers: 74.45.+c, 74.20.Rp, 74.50.+r

Introduction. The singlet superconductor (SSC) and ferromagnet (FM) phases are fundamentally incompatible, as the exchange field of the FM acts to align the anti-parallel spins of the electrons in singlet Cooper pairs, thus destroying the superconductivity [1]. Due to this pair-breaking effect, homogeneous coexistence of SSC and FM is very rare. On the other hand, SSC-FM interfaces can be readily fabricated in artificial layered heterostructures, and the study of these devices has attracted intense attention [2–7]. The pair-breaking effect is central to the understanding of these systems, e.g. it causes the spatial oscillation of the SSC correlations in the barrier of a ferromagnetic Josephson junction, which is responsible for the famed $0-\pi$ transition [2, 3]. It is well known that the FM suppresses the SSC gap close to the interface [2, 6, 7], and can induce a magnetization in the SSC [4]. Conversely, the SSC may influence the FM in order to minimize pair breaking, by suppressing the uniform magnetization near to the interface [4], or causing the spontaneous formation of domains in a thin FM layer so as to give zero averaged magnetization on the scale of the coherence length [5].

The coexistence of FM and triplet superconductor (TSC) states is more favorable, as the exchange field is only pair breaking when it is perpendicular to the Cooper pair spins. The physics of TSC-FM devices is therefore richer than their singlet counterparts, as the orientation of the FM moment relative to the TSC vector order parameter is now a crucial variable. This is predicted to control the nature of the proximity effect in TSC-FM bilayers [8] and the sign of the current in TSC-FM-TSC Josephson junctions [9]. In addition to this orientation-dependent pair breaking, the interface with the FM also induces distinctly new physics within the TSC [10, 11]: spin-flip reflection processes scatter the triplet Cooper pairs between the spin \uparrow and \downarrow condensates of the TSC, setting up a Josephson-like coupling between them. The resulting “spin Josephson effect” is manifested as a spon-

taneous spin current in the TSC normal to the TSC-FM interface [10], and is expected to contribute to the interface free energy [11]. The study of TSC-FM interfaces is timely, as the recent preparation [12] of superconducting thin films of Sr_2RuO_4 [13] opens the way to TSC heterostructures. Furthermore, the proposed appearance of Majorana fermions at TSC-FM interfaces in quantum wires motivates a deeper understanding of the interplay between FM and TSC [14].

In this letter we demonstrate that, contrary to what is expected from the pair-breaking effect, it is the orbital and not the spin component of the TSC order parameter which dictates the energetically-favorable orientation of the FM moment in a TSC-FM heterostructure. This reveals the emergence of a distinct form of *spin-orbital coupling* at TSC-FM interfaces, which originates from the spin-flip scattering of triplet Cooper pairs. We study a lattice model of a TSC-FM hybrid using a self-consistent Bogoliubov-de Gennes theory [6, 15], which accounts for the pair-breaking and spin-flip scattering processes on an equal footing. For a unitary p -wave TSC, we show that the latter stabilizes the FM moment either parallel or perpendicular to the spin orientation of the Cooper pairs, depending on the alignment of the p -wave gap with respect to the interface. For the chiral $p_x + ip_y$ state, increasing the strength of the FM exchange leads to a first order transition between these two configurations.

The model. We study a finite-size square lattice model of the planar TSC-FM heterostructure shown in Fig. 1(a). The lattice size is $L \times L$, with periodic boundary conditions imposed along the direction parallel to the interface. Indicating each site by a vector $\mathbf{i} \equiv (i_x, i_y)$, with i_x and i_y being integers ranging from $-L/2$ to $L/2$, we write the Hamiltonian

$$H = -t \sum_{\langle \mathbf{i}, \mathbf{j} \rangle, \sigma} (c_{\mathbf{i}\sigma}^\dagger c_{\mathbf{j}\sigma} + \text{H.c.}) - \mu \sum_{\mathbf{i}, \sigma} n_{\mathbf{i}\sigma}$$

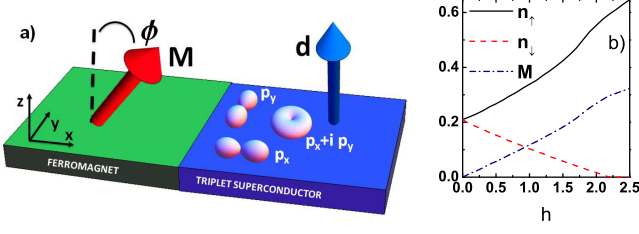


FIG. 1. (a) Schematic diagram of the two-dimensional TSC-FM junction. The FM region is located at $x < 0$, while the TSC is realized for $x > 0$. The magnetization **M** of the FM (big red arrow) forms an angle ϕ with the **d**-vector of the TSC (thin blue arrow), which defines the z axis. We study TSC states with p_x , p_y and $p_x + ip_y$ symmetry. (b) Evolution of the bulk FM magnetization and the majority and minority spin concentrations as a function of the exchange field h .

$$- \sum_{\langle \mathbf{i}, \mathbf{j} \rangle \in \text{TSC}} V (n_{i\uparrow} n_{j\downarrow} + n_{i\downarrow} n_{j\uparrow}) - \sum_{\mathbf{i} \in \text{FM}} \mathbf{h} \cdot \mathbf{s}_i, \quad (1)$$

where $c_{i\sigma}$ is the annihilation operator of an electron with spin σ at the site \mathbf{i} , $\langle \mathbf{i}, \mathbf{j} \rangle$ indicates nearest-neighbor sites, μ is the chemical potential, and $\mathbf{s}_i = \sum_{s,s'} c_{is}^\dagger \boldsymbol{\sigma}_{s,s'} c_{is'}$ is the spin density at site \mathbf{i} . The lattice is divided into three regions: the FM subsystem for $i_x < 0$, the TSC subsystem for $i_x > 0$, and the interface at $i_x = 0$. For simplicity, we assume that the hopping matrix element t is the same across the lattice; relaxing this assumption is not expected to qualitatively alter our results. All energy scales are expressed in units of t .

A nearest-neighbor attractive interaction $-V$ ($V > 0$) is present only on the TSC side of the junction. By tuning the electron density and pairing strength, at mean-field level this gives a TSC state with **d**-vector parallel to the z -axis, see Fig. 1(a). We consider three orbital symmetries: p_x , p_y , and $p_x + ip_y$. The interaction term in H is decoupled within the Hartree-Fock approximation by introducing the pairing amplitude on a bond $\Delta_{ij} = \langle c_{i\uparrow} c_{j\downarrow} \rangle$. The pairing amplitudes are used to construct the superconducting order parameter with the desired symmetry in the spin-triplet channel, which is then determined self-consistently [6, 15]. The $p_x + ip_y$ state (relevant for Sr_2RuO_4) is energetically most favorable as it fully gaps the 2D Fermi surface; anisotropic pairing interactions with $V_x = -V$, $V_y = 0$ and *vice versa* are used to model the p_x and p_y states, respectively. We choose the bulk TSC critical temperature to be $k_B T_c = 0.18$. The FM subsystem is modeled by the constant exchange field \mathbf{h} , which forms the angle ϕ with respect to the direction of the **d**-vector as shown in Fig. 1(a). Since the TSC state is invariant under spin rotations about the **d**-vector, \mathbf{h} is restricted to lie in the x - z plane, i.e. $\mathbf{h} = h(\sin(\phi), 0, \cos(\phi))$. The relation between the magnetization **M** and \mathbf{h} is shown in Fig. 1(b).

From the resulting mean-field Hamiltonian H_{MF} one can determine the condensation energy E_Δ of the TSC

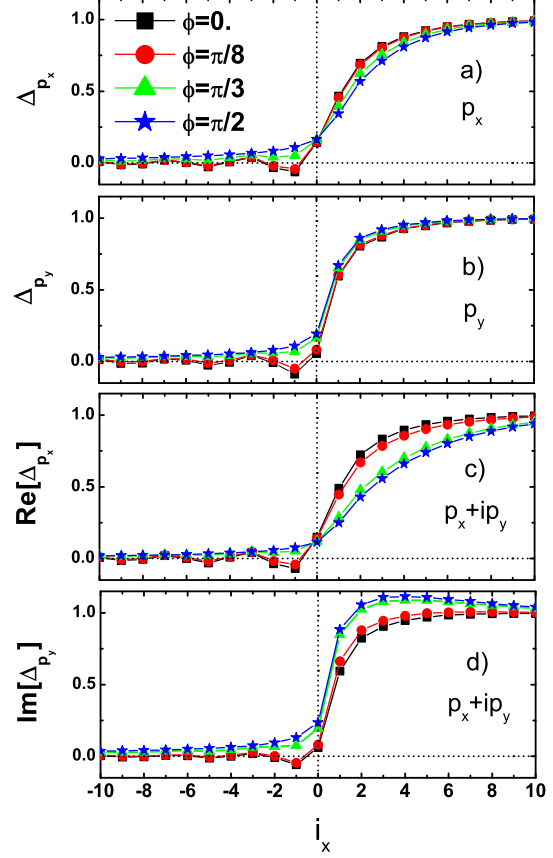


FIG. 2. Zero temperature pairing amplitude scaled to its bulk value as a function of the distance i_x from the interface at $h = 1.5$ and at different angles ϕ of the **d**-**M** misalignment. The spin-triplet orbital symmetry is of p_x (a), p_y (b), and chiral type (i.e. with a real p_x (c) and an imaginary p_y component (d)), respectively.

as well as the total Gibbs energy F of the junction:

$$E_\Delta = \frac{|V|}{L_x L_y} \sum_{\langle \mathbf{i}, \mathbf{j} \rangle \in \text{TSC}} |\Delta_{ij}|^2 \quad (2)$$

$$F = -\frac{1}{L_x L_y \beta} \ln(\text{Tr} \{ \exp[-\beta H_{MF}] \}) \quad (3)$$

where $\beta = (k_B T)^{-1}$. Both F and E_Δ depend on the exchange field and the angle ϕ through the self-consistent pairing amplitude and magnetization. The results presented here were obtained using $L = 120$; a larger lattice does not qualitatively change our conclusions.

Pairing amplitude. In Fig. 2 we present representative examples of the pairing amplitude profile near the interface for $h = 1.5$ and several different values of $0 \leq \phi \leq \frac{\pi}{2}$. Distinct trends are evident both in the FM and TSC sides of the junction as the exchange field is rotated from a parallel ($\phi = 0$) to a perpendicular ($\phi = \frac{\pi}{2}$) orientation with respect to the **d**-vector. Independent of the orbital sym-

metry, the proximity effect in the FM smoothly evolves from a monotonous decay to a damped oscillating behaviour as ϕ is decreased from $\frac{\pi}{2}$ to 0. The oscillating behaviour is similar to that observed in a SSC-FM junction and here it is also due to pair breaking, specifically the coupling of the z -component of the exchange field to the in-plane spin of the triplet Cooper pairs.

In contrast, the pairing amplitude on the TSC side of the interface strongly depends upon both the angle ϕ and the *orbital* symmetry of the TSC. Specifically, as can be seen in Fig. 2(a), a TSC with p_x orbital symmetry shows a reduction of the pairing amplitude close to the interface as the exchange field is tilted from parallel to perpendicular with respect to the \mathbf{d} -vector. For a p_y TSC we observe the opposite behaviour, although the effect is less pronounced [see Fig. 2(b)]. The chiral $p_x + ip_y$ TSC evidences both trends: decreasing ϕ from $\frac{\pi}{2}$ to 0 enhances the real (p_x) part of the gap [Fig. 2(c)], but suppresses the imaginary (p_y) part [Fig. 2(d)]. Interestingly, for a given exchange field magnitude h , the variation of each gap component of the $p_x + ip_y$ state with ϕ is much stronger than for the purely p_x or p_y state.

The pair-breaking effect on both the FM and the TSC side, which is the same for all orbital symmetries, cannot explain the different ϕ -dependence of the p_y and p_x gap profiles. This instead can be understood in terms of the spin-flip reflection of triplet Cooper pairs at the interface with the FM, which is also crucial for the spin Josephson effect [10, 11]. In such a scattering process, an incident Cooper pair with spin σ mutually perpendicular to \mathbf{d} and \mathbf{M} acquires the spin- and orbital-dependent phase shift $\pi - 2\sigma\phi + \Delta\theta$: the first two terms are due to the spin-flip, while the last is due to the phase change of the TSC gap upon specular reflection. Here $\Delta\theta = \pi$ (0) for the p_x (p_y) state, while $\Delta\theta$ depends on the angle of incidence for the $p_x + ip_y$ gap. It is well known that the gap is suppressed at interfaces where reflected Cooper pairs undergo a non-trivial phase shift [16]; by choosing ϕ so that the spin-flip reflected Cooper pairs have a $2\pi n$ phase shift, we hence expect to maximize the order parameter near the interface. Due to the different orbital phase shifts $\Delta\theta$, this occurs at $\phi = 0$ ($\frac{\pi}{2}$) for the p_x (p_y) pairing amplitude, in agreement with the numerics. This interplay of spin and orbital degrees of freedom reveals a novel type of spin-orbital coupling at the TSC-FM interface.

Stable moment orientation. The condensation energy E_Δ in the TSC depends upon the angle ϕ through the variation of the pairing amplitude near to the interface. In Fig. 3(a) we plot E_Δ as a function of ϕ for several typical cases. For the p_x and p_y gaps the energy is indeed maximized for the exchange field orientation which maximizes the gap amplitude. The $p_x + ip_y$ case is more complicated, since here the p_x and p_y gap components show opposite dependence upon ϕ . We find that the maximum in E_Δ shifts from $\phi = \frac{\pi}{2}$ to $\phi = 0$ with increasing exchange field strength. That is, for a weak FM

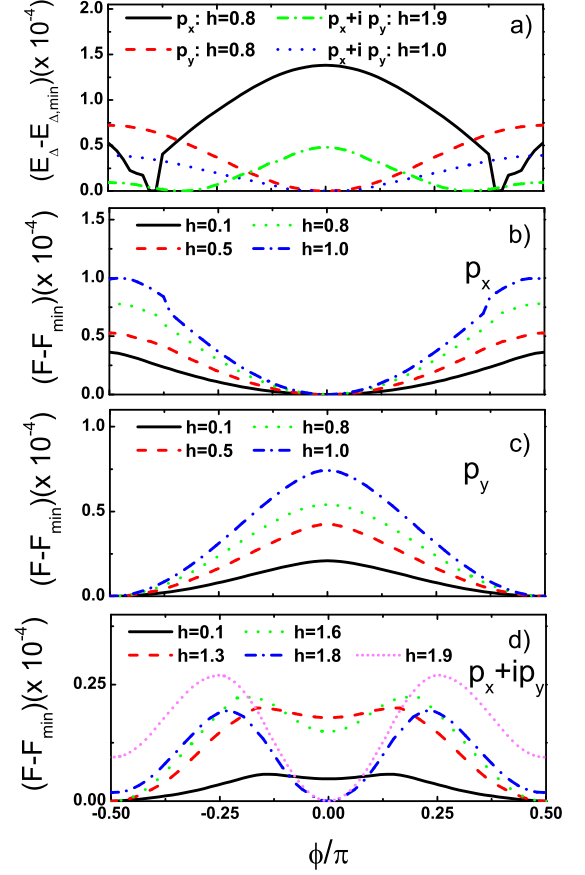


FIG. 3. (Color online) (a) Dependence of the condensation energy E_Δ on the angle ϕ . (b-d) Dependence of the Gibbs energy F on ϕ for various fixed h and for (a) p_x , (b) p_y and (c) $p_x + ip_y$ orbital symmetries of the spin-triplet superconductor. $E_{\Delta,\min}$ and F_{\min} are the minimum amplitudes of the related energies. All panels are for the temperature $T = 0.05$.

the p_y component dominates the physics, while at strong polarizations the p_x gap is most important.

The ϕ -dependent gain in condensation energy implies a favored orientation of the FM moment. This is determined from the Gibbs free energy F of the junction, which we plot in Fig. 3(b)-(d) for the three orbital symmetries as a function of ϕ . For the p_x orbital symmetry, the profile exhibits a single minimum at $\phi = 0$ and a maximum at $\phi = \pi/2$, and *vice versa* for the p_y TSC. In the upper panel of Fig. 4 we plot the difference $F(\phi = 0) - F(\phi = \frac{\pi}{2})$ between these points, which shows that the depth of the minimum monotonically increases with increasing exchange field h . The stable magnetic orientation is therefore parallel (perpendicular) to the \mathbf{d} -vector if the antinodes of the p -wave TSC gap are perpendicular (parallel) to the interface, see the sketch in the bottom panel of Fig. 4.

The Gibbs free energy for the $p_x + ip_y$ symmetry shows a competition between the tendency of the real and imag-

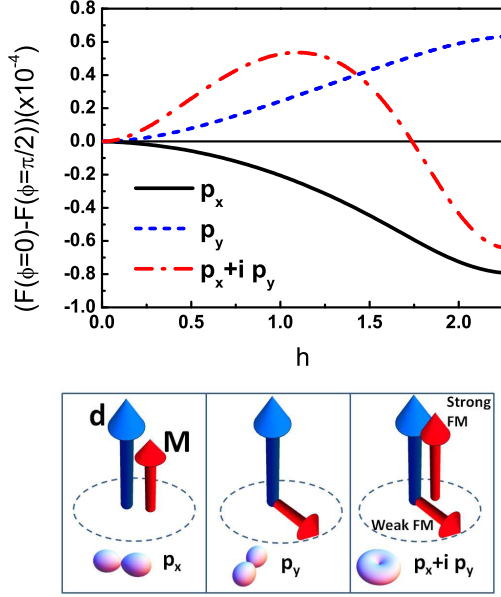


FIG. 4. (Color online) Top panel: Gibbs free energy difference between the parallel ($\phi = 0$) and perpendicular ($\phi = \frac{\pi}{2}$) configurations of the moment as a function of the exchange field strength h at temperature $T = 0.05$ for the p_x , p_y , and $p_x + ip_y$ TSCs. Bottom panel: sketch of the most favorable magnetic (red arrow) configurations with respect to the orbital symmetry and the \mathbf{d} -vector (blue arrow) of the TSC.

inary gap components to favour an FM with magnetization parallel and perpendicular to the \mathbf{d} -vector, respectively. This interplay produces minima in F at both $\phi = 0$ and $\phi = \frac{\pi}{2}$, with the exchange field strength selecting the stable state. As expected from the condensation energy, the $\phi = \frac{\pi}{2}$ state is the global minimum up to a critical exchange field $h_{cr,1}$ (≈ 1.74 at $T = 0.05$); the $\phi = 0$ state is stable up to a higher field $h_{cr,2}$ in the extreme half-metal regime (≈ 2.8 at $T = 0.05$, not shown in Fig. 4). $h_{cr,1}$ and $h_{cr,2}$ merge together as the temperature is increased, so that only the $\phi = \frac{\pi}{2}$ configuration is stable sufficiently close to T_c . We note that the competition between the two gap components is expected to be dependent upon the details of the system.

Our results imply a close connection between the spin-orbital coupling and the spin Josephson effect in the TSC-FM junction [10, 11]. Specifically, the spin current in the Josephson effect is generated by a ϕ -dependent Helmholtz free energy; for a non-self-consistent model of a thin FM layer on a bulk TSC, the free energy due to the interface electronic reconstruction has similar form to that obtained here, and gives the same stable magnetization configurations for the p_x and p_y states [11].

Experimental considerations. Although the energy difference between the $\phi = 0$ and $\frac{\pi}{2}$ states shown in Fig. 4 is very small, this results from averaging what is essentially an interface effect over the entire lattice; the energy gain per interface unit cell is L times larger, and gives an

anisotropy energy on the order of $\sim 0.01 k_B T_c$ for the microscopic parameters chosen here. In the case of a thin FM layer of width a few unit cells, this is comparable to free energy change due to electronic reconstruction within the FM itself [11]. The magnetic anisotropy induced by the coupling to the TSC could be observed by ferromagnetic resonance (FMR) measurements: for an exchange field $h = 0.5$ in the FM, and choosing Sr_2RuO_4 ($T_c = 1.5\text{K}$) for the bulk TSC, we estimate a precession frequency of $\sim 5 \cos(\alpha)$ GHz. Since there is no spin-orbital coupling at SSC-FM interfaces, the observation of this precession would strongly indicate a TSC state in the superconductor. For a thicker FM layer, we speculate that the spin-orbital coupling could modify the magnetization profile near the interface, effectively creating a spin-active boundary layer, which can greatly influence the proximity effect in the FM [7].

For the purposes of simplicity we have neglected complicating factors such as intrinsic anisotropy of the FM, demagnetization effects, spin-orbit coupling, etc. Including these requires a more elaborate description, but does not change the basic physics of the TSC-FM interface discussed here. Some of these effects may even be turned to our advantage, e.g. to observe the appearance of the anisotropy axis due to the spin-orbital coupling, it would be favorable to select an FM with biaxial easy axes oriented perpendicular and parallel to \mathbf{d} .

Conclusions. In this letter we have evidenced a novel type of spin-orbital coupling which appears at TSC-FM interfaces. Specifically, an FM moment parallel (perpendicular) to the TSC \mathbf{d} -vector maximizes the magnitude of a p -wave order parameter with antinodes perpendicular (parallel) to the interface. The origin of this spin-orbital coupling is ascribed to the spin-flip reflection of Cooper pairs at the TSC-FM interface. We have determined the lowest-energy magnetic configuration by calculating the Gibbs free energy. Our method allows us to treat many different interface physics on an equal footing, e.g. the proximity effect, the interfacial electronic reconstruction and the superconducting order parameter variation. We show that the latter is most important, due to the change in the condensation energy of the TSC. For the chiral TSC, where both types of p -wave gaps are present, the stable moment orientation switches between the perpendicular and parallel configurations with increasing exchange field. The coupling causes the appearance of an anisotropy axis in the FM which could be observed in FMR measurements, and can act as a test of the orbital and spin pairing state of the TSC.

The authors thank M. Sigrist and C. Timm for useful discussions. The research leading to these results has received funding from the EU -FP7/2007-2013 under grant agreement N. 264098 - MAMA.

-
- [1] D. Saint-James, D. Sarma, and E. J. Thomas, *Type II Superconductivity* (Pergamon, New York, 1969).
 - [2] A. I. Buzdin, Rev. Mod. Phys. **77**, 935 (2005); F. S. Bergeret, A. F. Volkov, and K. B. Efetov, *ibid.* **77**, 1321 (2005).
 - [3] V. V. Ryazanov *et al.*, Phys. Rev. Lett. **86**, 2427 (2001).
 - [4] F. S. Bergeret, A. F. Volkov, and K. B. Efetov, Phys. Rev. B **69** 174504 (2004).
 - [5] A. I. Buzdin and L. N. Bulaevskii, Sov. Phys. JETP **67**, 576 (1988); F. S. Bergeret, K. B. Efetov, and A. I. Larkin, Phys. Rev. B **62**, 11872 (2000).
 - [6] M. Cuoco, A. Romano, C. Noce, and P. Gentile, Phys. Rev. B **78**, 054503 (2008).
 - [7] M. Eschrig and T. Löfwander, Nature Phys. **4**, 138 (2008); J. Linder, M. Cuoco, and A. Sudbø, Phys. Rev. B **81**, 174526 (2010).
 - [8] G. Annunziata *et al.*, Phys. Rev. B **83**, 060508(R) (2011).
 - [9] P. M. R. Brydon and D. Manske, Phys. Rev. Lett. **103**, 147001 (2009); B. Bujnowski, C. Timm, and P. M. R. Brydon, J. Phys.: Condens. Matter **24**, 045701 (2012).
 - [10] P. M. R. Brydon, Phys. Rev. B **80**, 224520 (2009).
 - [11] P. M. R. Brydon, Y. Asano, and C. Timm, Phys. Rev. B **83** (2011).
 - [12] Y. Krockenberger *et al.*, Appl. Phys. Lett. **97**, 082502 (2010).
 - [13] A. P. Mackenzie and Y. Maeno, Rev. Mod. Phys. **75**, 657 (2003).
 - [14] Y. Oreg, G. Refael, and F. von Oppen, Phys. Rev. Lett. **105**, 177002 (2010); L. Jiang *et al.*, *ibid.* **107**, 236401 (2011).
 - [15] K. Kuboki and H. Takahashi, Phys. Rev. B **70**, 214524 (2004).
 - [16] L. J. Buchholtz and G. Zwicknagl, Phys. Rev. B **23**, 5788 (1981); C. Bruder, Phys. Rev. B **41**, 4017 (1990).